AN EFFICIENT SPLIT-STEP DIGITAL FILTERING

METHOD IN SIMULATING PULSE PROPAGATION

WITH POLARIZATION MODE DISPERSION

EFFECT

AN EFFICIENT SPLIT-STEP DIGITAL FILTERING

METHOD IN SIMULATING PULSE PROPAGATION

WITH POLARIZATION MODE DISPERSION

EFFECT

By

KAN HE, B. Eng. Wuhan University

A thesis
submitted to the school of graduate studies
in partial fulfillment of the
requirement for the degree of
Master of Applied Science
In
Electrical Engineering

Hamilton, Ontario, Canada, 2007

MASTER OF APPLIED SCIENCES (2007)   MCMASTER UNIVERSITY

(Electrical and Computer Engineering)   Hamilton, Ontario

TITLE: An Efficient Split-Step Digital Filtering Method in Simulating Pulse Propagation with Polarization Mode Dispersion Effect

AUTHOR: Kan He, B. Eng. Wuhan University

SUPERVISOR: Dr. Xun Li, Department of Electrical and Computer Engineering

NUMBER OF PAGES: vi, 58

Acknowledgements

I would like to express my special thanks to my supervisor Dr. Xun Li for his kind guidance and great support on my research, and his belief in me from the very beginning. I also would like to thanks Dr. Shiva Kumar and Dr. Chang-Qing Xu, they gave a lot of good advises on my thesis and research. Thanks to Dr. Wei-Ping Huang for his excellent teaching on the fundamentals of this area and I learned a lot from his courses. Thanks to Dr. Jim Reilly who teaches me what is the right attitude towards a serious science. Thanks to Cheryl Gies who offers her kind assistance to help me accomplish my graduate study.

Thanks to all of my friends in photonics group. I will always remember the days I spent with you. Also sincerely thanks to all the people who had helped me in Canada.

Finally, I would like to thank my parents. Their encouragement pushed me through those hardest days. They let me know how great can parents be and what is the most important thing in my life.

Abstract

The rapid increasing bandwidth requirement of communication systems demands powerful numerical simulation tools for optics fiber. The computational efficient, memory saving and stable are of the most important characteristics for any simulation tools used for long-haul and broadband optics fiber. An optimized split-step digital filtering method is developed in this paper. The concept of Fourier integral and Fourier series are used in extracting a FIR filter which is used to fit the original transfer function. A further optimization process which employs windowing technique to improve computation efficiency had also been done. Compared with split-step frequency method, our method improves the computation efficiency. Only simple shifts and multiplications are needed in our method. This optimized digital filtering method differs from the former digital filtering method in a sense that the filter length of the FIR filter we extracted is reduced to a very small number. The computation time can be saved as much as 96% than before. This method can also be used to solve coupled nonlinear Schrodinger equation which governs polarization mode dispersion effect in fibers. A new simulation scheme for PMD is proposed to save computation time. The propagation results shows good accordance to those already published results.

Table of Contents

Chapter 1

Introduction

1.1 Simulation of Optics Communication Systems

With the growth of internet and data traffic, there is an increasing demand on the bandwidth of communication systems. The wavelength-division multiplexing (WDM) system is introduced as WDM systems multiplexes channels in different wavelength in a single optic fiber. But with the accumulation effects of chromatic dispersion and fiber nonlinearity, limitations will appear in the propagation of input signals. In order to simulate the communication systems as accurate as possible, investigations on these limitations are necessary. The optic fiber is a very important part of communication systems. And for the fact that the main limitations in optics communication system, such as chromatic dispersion, nonlinear effect and polarization mode dispersion, are brought in by optic fiber [3][5]. The simulation of signal propagation in optic fiber becomes important in the present communication system simulation.

The governing equation that describes the pulse propagation in optics fiber is nonlinear Schrodinger equation (NSE). The NSE is a nonlinear partial differential equation that does not have analytical solution, except under some specific conditions where inverse scattering method can be used. Solving the NSE numerically is crucial for simulating the pulse propagation in fiber.

The split-step method is widely used in solving the NSE that describes the pulse propagation in optics fiber. The advantage of the split-step method is efficiency and stability, as well as its conceptual clarity. Traditionally, the split-step is implemented in frequency domain. With the use of fast Fourier transformation (FFT), the computation speed of split-step frequency domain method is improved. The operational flip-flop for this method on a frame is $O(N \log N)$, where N is the sampling points of input signal in a frame. There are also some efforts to improve the efficiency and accuracy of the split-step method [4][10][15]. The most recent progress is published in [20].

There is a drawback with all the above methods, that is, the input sampling data must be processed simultaneously. In order to deal with ultra-short pulse [20] and multi-channel WDM systems, a very small sampling interval must be chosen. Hence, the input sampling points of a frame N will be very large. Hence, the computation time will be even large. When the input signal expands to the edges of computation window, an oscillation effect will appear at two edges of signal, which is called the aliasing effect. In order to eliminate the aliasing effect, a further anti-aliasing step must be employed to solve the NSE accurately, that is, selects a larger time domain window which gives sufficient frequency resolution. All those process requires increased computation time. The computation efficiency is hence reduced.

A split-step time domain method using digital filtering technique is developed in [1].A FIR filter is extracted with the error over the entire frequency domain been controlled.

The split-step time domain computational structure is also given, with only simple shifts and multiplications are included in this calculation [1]. The computation cost of this method is hence reduced due to the shortened length of the extracted digital filter.

1.2 Polarization Mode Dispersion

The PMD effect is caused by the fiber birefringence that makes the difference of propagation speed between fiber polarization modes, which randomly spreads the optical pulse as both the fiber birefringence and orientation angles are random. The PMD effect is accumulated in the process of pulse propagation and limits the data transmission rate of communication systems. The longer the propagation distance is, the stronger the PMD effect may be observed at the receiver.

With the long-haul fiber is widely used in the present transmission systems, the simulation of polarization mode dispersion (PMD) effect became more and more important. By solving the coupled nonlinear Schrodinger equation (CNSE) that governs the PMD in optics fiber, the PMD effect can be simulated. Both the split-step frequency method and digital filtering method can be used to solve the CNSE. The same situation as the NSE case, try to increase the computation efficiency will be a major concern for the simulation of PMD.

1.3 Motivation of this work

The computation cost of former digital filtering method is very large, for the fact that the filter length of the extracted filter is fixed to a maximized number that guarantee the accuracy in the bandwidth. The larger filter length increases the computation cost of this simulation. In order to make this digital filtering method more effective, we need to find a better way to extract the FIR filter, to make the filter length reduced to a smaller number without much sacrifice in accuracy. In order to further improve the computation efficiency of this digital filtering method in the simulation of PMD, we also want to find a better computation scheme that can take advantage of the extracted digital filters.

In our paper, an optimized digital filtering method is proposed with the concept of Fourier series. In order to reduce the oscillation effect (Gibbs phenomenon) that is caused by reducing the truncation number of the filter length, the windowing method is further applied. The comparison of results shows this optimized digital filtering method has better computation efficiency than the former method. A new simulation scheme for the PMD effect is also proposed. The simulation results show good agreement between our proposed scheme and conventional split-step frequency method using FFT.

1.4 Thesis Organization

This thesis is organized as follows. The basic propagation equations including nonlinear Schrodinger equation and coupled nonlinear Schrodinger equation are presented in chapter 2. In chapter 3, the conventional computation model for split-step digital filtering method is showed. Then, the optimized split-step digital filtering method is proposed in

chapter 4. Both models for NSE and CNSE are included in the above two chapters. In chapter 5, some implementation details are described. And in chapter 6, the simulation results are showed with comparison between digital filtering method and frequency domain method. A good agreement can be observed for both NSE and CNSE. The last chapter of the thesis is conclusion.

Chapter 2

Numerical Model

2.1 Nonlinear Schrodinger Equation

It's the wave equation that describes the optical field propagation in the optic fiber. From wave equation, we can derive the nonlinear Schrodinger equation (NSE) which governs the slow-varying envelope of the optical field. The NSE is given as the following:

$$\frac{\partial \overline{A}(z,t)}{\partial z} + \frac{\alpha}{2}\overline{A}(z,t) + \beta_1 \frac{\partial \overline{A}(z,t)}{\partial t} + i\frac{\beta_2}{2}\frac{\partial^2 \overline{A}(z,t)}{\partial t^2} - \frac{\beta_3}{6}\frac{\partial^3 \overline{A}(z,t)}{\partial t^3} = i\gamma \left|\overline{A}(z,t)\right|^2 \overline{A}(z,t) \quad (1)$$

Where $\overline{A}$ denotes the slow-varying envelop of the optical field, β_1 is the wave propagation constant, β_2 and β_3 is the second and third order dispersion coefficients, respectively. α is the fiber loss and γ is fiber nonlinear parameter. i is the imaginary unit. Here, we neglect the dispersions higher than third order.

We can further exclude the time spent on propagation at the group velocity v_g from the real time, by use a new reference time $T = t - \beta_1 z$, where $\beta_1 = \frac{1}{v_g}$. Hence the third term in (1) with β_1 can be excluded.

In order to rescale the envelope to count the fiber loss explicitly, we can

set $\overline{A}(z,T) = A(z,T)e^{-\frac{\alpha}{2}z}$. The nonlinear Schrodinger equation hence becomes [1]:

$$\frac{\partial A(z,T)}{\partial z} + i\frac{\beta_2}{2}\frac{\partial^2 A(z,T)}{\partial T^2} - \frac{\beta_3}{6}\frac{\partial^3 A(z,T)}{\partial T^3} = i\gamma e^{-\alpha z}\left|A^2(z,T)\right|A(z,T) \tag{2}$$

2.2 Coupled Nonlinear Schrodinger Equation

When fiber birefringence becomes a major concern, we need a set of equations which

counts for the polarization effect of propagation in optic fiber [5]. The coupled nonlinear

Schrodinger equation (CNSE) can be employed to describe this polarization effect. The

CNSE can be showed as following [2][22]:

$$\frac{\partial}{\partial z}\overline{U} + \frac{\alpha}{2}\overline{U} - ib\Sigma\overline{U} + b'\Sigma\frac{\partial}{\partial T}\overline{U} + i\frac{\beta_2}{2}\frac{\partial^2}{\partial T^2}\overline{U} - \frac{\beta_3}{6}\frac{\partial^3}{\partial T^3}\overline{U} - i\gamma\left|\overline{U}\right|^2\overline{U} + \gamma\frac{i}{3}\left(\overline{U}^\dagger\sigma_2\overline{U}\right)\sigma_2\overline{U} = 0 \tag{3}$$

In the above equations, $\overline{U}$ denotes the complex envelope of two polarizations of the

optical field in fiber $\begin{bmatrix}\overline{U}_1\\\overline{U}_2\end{bmatrix}$ and $\overline{U}^\dagger$ is $\begin{bmatrix}\overline{U}_1^*, \overline{U}_2^*\end{bmatrix}$. Σ is the matrix $\begin{bmatrix}\cos\theta & \sin\theta\\\sin\theta & -\cos\theta\end{bmatrix}$ and σ_2

is the matrix $\begin{bmatrix}0 & -i\\i & 0\end{bmatrix}$.

As we showed for the NSE, T is the new reference time $T = t - \beta_1 z$, which facile us to view the signal propagating in a limited duration time window. b is the birefringence strength which is defined as $b = \dfrac{\pi}{\Lambda_{beat}}$, Λ_{beat} is beating length of the fiber. b' is given as

$b' = \dfrac{D_{PMD}}{2(2L_{corr})^{\frac{1}{2}}}$, where D_{PMD} is the polarization mode dispersion coefficient, and L_{corr} is the fiber correlation length. θ is the orientation angle. Here, optic fiber is viewed as linked segments, in which the length is small enough that the fiber birefringence can be seen as constant among each sub-segment [2]. In each sub-segment, the fiber birefringence is pre-determined, which means the coupling between two polarizations occurs only between these segments, not within these segments.

And as in the equation (1), β_2 and β_3 are the second and third order dispersion coefficients, respectively. α is the fiber loss and γ is fiber nonlinear parameter. i is the imaginary unit. Here, we neglect the dispersions higher than third order.

The equation (3) describes the PMD effect in the optic fiber. As we showed on the equation (1), we can further modify equations (3) to explicitly count the loss by setting: $\overline{U} = U e^{-\frac{\alpha}{2}z}$. Hence, the equations (3) become:

$$\frac{\partial}{\partial z}U - ib\Sigma U + b'\Sigma\frac{\partial}{\partial T}U + i\frac{\beta_2}{2}\frac{\partial^2}{\partial T^2}U - \frac{\beta_3}{6}\frac{\partial^3}{\partial T^3}U - i\gamma e^{-\alpha z}|U|^2 U + \gamma\frac{i}{3}e^{-\alpha z}\left(U^\dagger\sigma_2 U\right)\sigma_2 U = 0 \quad (4)$$

On the left side of the above equation (4), the second term and the third term is the contribution of the fiber birefringence on the input signal. The fourth and fifth terms count the second and third order dispersions. And the sixth term is the fiber nonlinear effect. The last term on the left side of the above equations counts the coupling effect between the two polarization modes in fiber. The power exchange of the two polarization modes are linked via this term. In mathematical view, the coupling effect of the two polarization modes can be expressed through a transfer matrix.

Chapter 3

Conventional Solution Scheme

3.1 Split-Step Frequency Domain Method

The basic idea of spilt-step method [4] is to separate the linear and the nonlinear operators and solve them alternatively to get the solution of the nonlinear Schrodinger equation. The equation (2) can be written as:

$$\frac{\partial A}{\partial z} = (D + N)A \tag{5}$$

where D is the linear operator and N is the nonlinear operator. The linear operator D counts the dispersion effect which includes second order and third order dispersion. The nonlinear operator N counts the nonlinear effects in the fiber. They can be expressed as:

$$D = -i\frac{\beta_2}{2}\frac{\partial^2}{\partial T^2} + \frac{\beta_3}{6}\frac{\partial^3}{\partial T^3} \tag{6}$$

$$N = i\gamma e^{-\alpha z}|A|^2 \tag{7}$$

The above two operators effect alternatively over a propagation distance Δz , which means the linear and nonlinear take effects separately and alternatively. So the calculation takes place in two steps. In the first step, only the linear dispersion effects,

while N=0. Then, in the second step, only the nonlinear part effects, which means D=0. Hence, the process can be expressed as following:

$$A(z+\Delta z,\omega) = H_D F[A(z,T)]$$ (8)

$$A(z+\Delta z,T) = \exp(i\Delta z\gamma e^{-\alpha z} \left| F^{-1}[A(z+\Delta z,\omega)] \right|^2) \times F^{-1}[A(z+\Delta z,\omega)]$$ (9)

In the above equations, $F[\ ]$ represents Fourier transformation which transfers the signal from time domain to frequency domain. $F^{-1}[\ ]$ represents inverse Fourier transformation.

In equation (8), H_D is the fiber transfer function in frequency domain:

$$H_D(\omega) = \exp[i(\frac{1}{2}\beta_2\Delta z\omega^2 - \frac{1}{6}\beta_3\Delta z\omega^3)]$$ (10)

The split-step frequency method is accomplished from the equations (8), (9). The consequence can be showed as following:

Step 1: This method first converts the input signal from time domain to frequency domain using FFT in position z.

Step 2: Only considering the linear dispersion, and then multiply the input signal with the fiber transfer function H_D in frequency domain, to let the signal propagating a distance Δz to the position $z + \Delta z$ with only the linear dispersion presents.

Step 3: Using inverse Fourier transformation to convert the propagated signal from frequency domain to time domain in the position $z + \Delta z$. Then implement equation (9) to get the nonlinear effect applied on the propagated signal in the position $z + \Delta z$ in time domain.

Following the above steps, the input signal can be propagated in the optic fiber through solving nonlinear Schrodinger equation in a distance Δz, with both linear dispersion and nonlinear effect applied. By repeat this process, any given propagation distance can be achieved.

3.2 Split-Step Frequency Domain Method for CNSE

The split-step frequency method on coupled nonlinear Schrodinger equation is similar to the method applied on nonlinear Schrodinger equation [2] [6]. But we have to use this method to solve a different equation (4), instead of NSE.

First, we still need to separate the linear and nonlinear part of the equations (4) as following:

$$\frac{\partial}{\partial z}U = (D+N)U \tag{11}$$

where D is the linear operator counts for the linear dispersion. $N = \begin{bmatrix} N_1 \\ N_2 \end{bmatrix}$ is the nonlinear

operators for the two different polarizations in the fiber, respectively. These terms can be

expressed as:

$$D = -i\frac{\beta_2}{2}\frac{\partial^2}{\partial T^2} + \frac{\beta_3}{6}\frac{\partial^3}{\partial T^3} \tag{12}$$

$$N = i\gamma e^{-\alpha z}[|U|^2 - \frac{1}{3}(U^\dagger \sigma_2 U)\sigma_2] \tag{13}$$

Just like the process applied on NSE, the linear dispersion operator D and nonlinear

operator N takes effect alternatively over a small propagation distance Δz. It means we

treat the linear dispersion and nonlinear effect separately. The split-step frequency

method on CNSE is carried out in two steps: linear step and nonlinear step.

For the linear step, we only consider the linear step, and then the equations (4) can be

expressed as:

$$\frac{\partial}{\partial z}U = ib\Sigma U - b'\Sigma\frac{\partial}{\partial T}U + DU \tag{14}$$

13

Apply Fourier transformation on the above equation to transfer both sides to frequency domain, we can get:

$$\frac{\partial}{\partial z}U = ib\Sigma U - i\omega b'\Sigma U + DU \tag{15}$$

where $D = i\frac{\beta_2}{2}\omega^2 - i\frac{\beta_3}{6}\omega^3$, which is the linear dispersion operator in frequency domain.

U is the polarizations envelope in frequency domain.

The solution to equation (15) can be expressed as [2]:

$$U(z + \Delta z, \omega) = \exp(D\Delta z)MU(z, \omega) \tag{16}$$

In the above equation (22), the 2×2 matrix $M(z, \omega)$ counts for the fiber birefringence effect. We mentioned before we can view the propagation distance Δz is composed of a number of sub-segments δz, within which the fiber birefringence can be seen as constant. The fiber birefringence only takes effect between these sub-segments. Hence the transfer matrix $M(\omega)$ is constant within each sub-segments δz, but varies randomly between these sub-segments as the fiber birefringence is a random effect in optic fiber. In each sub-segments δz, the transfer matrix can be expressed as:

$$m_j = \begin{bmatrix} m_{11}^j & m_{12}^j \\ m_{21}^j & m_{22}^j \end{bmatrix} \tag{17}$$

where:

$$m_{11}^j = m_{22}^{j\,*} = \cos[(b - b'\omega)\delta z] + i\cos(\theta_j)\sin[(b - b'\omega)\delta z] \tag{18}$$

$$m_{12}^j = m_{21}^j = i\sin(\theta_j)\sin[(b - b'\omega)\delta z] \tag{19}$$

The total transfer matrix $M(\omega)$ that counts all the sub-segments can be expressed as:

$$M(\omega) = \prod_{j=1}^{N} m_j(\omega) \tag{20}$$

where N is the total number of sub-segments.

In the equations (18) and (19), b is the fiber birefringence strength. θ_j is the orientation angle. The value of θ_j is constant in each sub-segments, but different between sub-segments.

There are two models to capture the randomness of the fiber birefringence. The first model is to set the birefringence orientation varies randomly from each sub-segments, with birefringence strength is fixed. While the second model is to set both the fiber

birefringence orientation and strength varies randomly between each sub-segments. And it's been shown that both of these two models lead to an identical result [8]. In this paper, the first model is chosen because it's easier to treat and hence lower the computation complexity.

For the nonlinear step, the CNSE only with nonlinear term can be expressed as:

$$\frac{\partial}{\partial z} U = NU \tag{21}$$

From the above equations, we can get:

$$\overline{\overline{U}}(z + \Delta z, T) = \exp(\Delta z N)\overline{U}(z + \Delta z, T) \tag{22}$$

In the above equations, N is shown in equations (13). $\overline{U}$ is the envelope which experienced linear effect but did not experience nonlinear effect yet. And $\overline{\overline{U}}$ is the envelope which also counts the nonlinear effect.

The split-step frequency method for the simulation of coupled nonlinear Schrodinger equation can be implemented through solving the equations (16) and (22) alternatively, to let the input signal propagate any given distance.

Chapter 4

Time Domain Solution Scheme

4.1 Split-Step Digital Filtering Method

In order to avoid the transformation between time domain and frequency domain, we need to solve the NSE only in time domain. Here we bring in a nouveau method using the digital filtering concept to solve the NSE in time domain, while requires less computation cost than other methods.

We first build a polynomial function which can be viewed as a FIR filter in frequency domain [9]:

$$H_F(\omega) = \sum_{k=-M}^{M} h_k \, e^{ik\Delta\omega} \tag{23}$$

In the above equation, Δ is the sampling interval in time domain. h_k with k=-M to M is the filter coefficients that will be determined later. 2M+1 is the total number of the filter coefficients, which we also call it filter length. The computation cost is depending on the number of 2M+1, which we will discuss later.

The FIR filter $H_F(\omega)$ should be approximates to the frequency domain fiber transfer function $H_D(\omega)$ in the bandwidth as much as possible, and the portion outside the bandwidth we are interested in is not important in our case, so we can make it a periodic function. The reason will be discussed later.

The expression of $H_D(\omega)$ is showed in equation (10). It is obvious that the filter length 2M+1 have to be infinite, in order to make $H_F(\omega)$ fitted to $H_D(\omega)$ as much as possible. But it is impossible to make the filter length infinite in the implementation. Hence we have to make the number of 2M+1 as large as possible to make the error between $H_F(\omega)$ and $H_D(\omega)$ smaller [9]. But with the increasing of filter length, the computation cost will increase too, which is not desirable in the simulation [10]. So try to decrease the number of filter length 2M+1, while keep the error between original fiber transfer function $H_D(\omega)$ and our fitted FIR filter $H_F(\omega)$ as small as possible, become the major concern in split-step digital filtering method.

Here we propose a nouveau scheme which use the concept of Fourier transformation, combined with windowing technique, to approximate the fitted function $H_F(\omega)$ to original function $H_D(\omega)$. Considering the polynomial function format of

$H_F(\omega) = \sum_{k=-M}^{M} h_k \, e^{ik\Delta\omega}$, we find it has a similar expression as the Fourier series [11] if M is

infinite. From the definition of Fourier transformation, we can derive the equation that will calculate the filter coefficients h_k [9]:

$$h_k = \frac{1}{\omega_B} \int_{-\frac{\omega_B}{2}}^{\frac{\omega_B}{2}} H_D(\omega) e^{-ik\Delta\omega} d\omega \qquad (24)$$

In the above equation, ω_B is the effective bandwidth which is determined by the spectrum of the input signal [9] [12]. From the equations (23) and (24), we can see that this process is similar to the process of Fourier transformation. The only difference is k in equation (23) should be from infinite minimum to infinite maximum for Fourier transformation. But in our case, k only has a limited number. The limit number of k is the source of fitting error introduced between $H_F(\omega)$ and $H_D(\omega)$.

The reason why we place $H_D(\omega)$ in equation (24) is that we need to approximate $H_F(\omega)$ to $H_D(\omega)$. Even though the original transfer function $H_D(\omega)$ is infinite [5], we are only interesting in the original transfer function in the effective bandwidth ω_B. The fitted transfer function is then produced as periodic function, which takes ω_B as its period and has identical amplitude and phase to within each period. Namely, $H_F(\omega)$ equals to $H_D(\omega)$ in the effective bandwidth $(-\omega_B/2, \omega_B/2)$, and this shape repeats in other periods: ..., $(-3\omega_B/2, -\omega_B/2)$, $(\omega_B/2, 3\omega_B/2)$, ... of $H_F(\omega)$.

In our case, there is no difference of amplitude between $H_F(\omega)$ and $H_D(\omega)$ throughout the frequency domain, i.e., $|H_F(\omega)| = |H_D(\omega)| = 1$. But the phase of $H_F(\omega)$ and $H_D(\omega)$ will be different outside the effective bandwidth $(-\omega_B/2, \omega_B/2)$, the phase of $H_D(\omega)$ will extent with frequency domain as what it is, while the phase of $H_F(\omega)$ will repeat what it is like within the effective bandwidth.

The amplitude and phase of the original function and fitted function is shown in Fig. 1 as below:
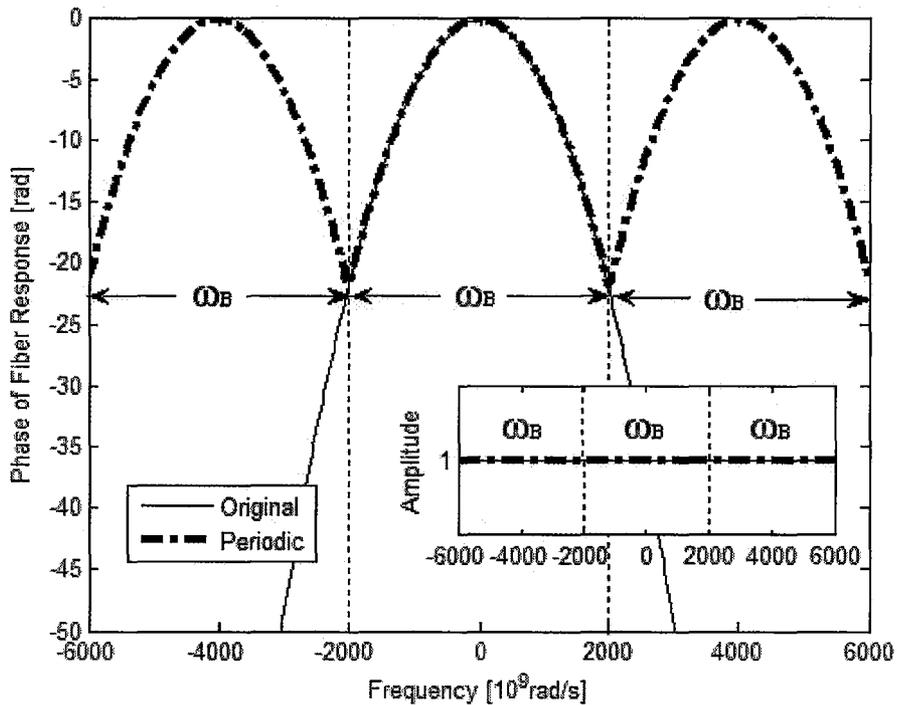
Fig. 1 The amplitude and phase of original function and fitted FIR filter.

In the figure 1, we see that the response of fitted function is a periodic function, just as we discussed before. The portion of agreement with original function within the bandwidth ω_B is guaranteed.

We can then replacing $H_D(\omega)$ by $H_F(\omega)$ in equation (8):

$$A(z+\Delta z,\omega) = \sum_{k=-M}^{M} h_k e^{ik\Delta\omega} A(z,\omega) \tag{25}$$

Transforming the above equation back to time domain [13], we get:

$$A(z+\Delta z,T) = \sum_{k=-M}^{M} h_k A(z,T-k\Delta) \tag{26}$$

The above equation (26) together with equation (9) which counts the nonlinear effect in optic fiber, form the split-step time domain digital filtering method. Only simple multiplications and shift summations are involved. Hence eliminate the process of transformation between time domain and frequency domain.

We assume that the input signal sampling points is N and the filter length is 2M+1. The operational flip-flop of our method for each propagation step is proportional to $O((2M+1)N)$, while the operational flip-flop of split-step frequency method is

$O(\text{NlogN})$ [1]. We can see that as long as $2M+1 < \log N$, our method will be more computational efficient than the split-step frequency method. And in the present communication systems, the input sampling points N of a frame can be very large as we discussed before. So the optimized digital filtering method requires less computation time than split-step frequency method when $2M+1 < \log N$.

In the former digital filtering method for the split-step time domain method [1], the linear least-square method is employed to approximates $H_F(\omega)$ to $H_D(\omega)$. The advantage of this linear least-square method is guaranteed accuracy in the entire bandwidth ω_B. But the filter length of the formal digital filtering method is maximize and fixed in order to keep the error within the entire bandwidth minimized. The computation time is hence becoming extremely large.

In the later implementation part, we will show that our method needs much less filter length than the former split-step digital filtering method. With the increasing of sampling points of input signal, this advantage will largely improve the computation efficiency of the former split-step method.

4.2 Split-Step Digital Filtering Method for CNSE

The digital filtering method can also be implemented on coupled nonlinear Schrodinger equation which counts the PMD effect. Here, we propose a nouveau computation scheme to save the computation cost without loss the randomness of fiber birefringence.

The key idea of this new scheme is to extract the fitted FIR filter coefficients for a large number of transfer matrices $m(\omega)$ at the very beginning and just need to do once. The birefringence orientation angle will vary randomly between each sub-segment. So we first assume a large number of orientation angles, and then use these angles to construct the elements of transfer matrices $m(\omega)$ that cover each sub-segment δz. The next step is to extract the digital filters corresponding to these transfer matrices. Firstly, the input signal will be propagating through a number of sub-segments filters to cover a propagation step Δz. Then the input signal will be propagated through the dispersion filter that is extracted in the last section. The last step will be performing the nonlinear effect on the input signal. By following the above routine, the randomness of fiber birefringence is guaranteed. The fitted FIR filters are only needed to be extracted once in the very beginning. The computation cost is hence saved. The detailed computation scheme is showed as following:

At first, we assume four FIR filters $\sum_{k=-M}^{M} h_k^{(11)} e^{ik\Delta\omega}$, $\sum_{k=-M}^{M} h_k^{(12)} e^{ik\Delta\omega}$, $\sum_{k=-M}^{M} h_k^{(21)} e^{ik\Delta\omega}$ and

$\sum_{k=-M}^{M} h_k^{(22)} e^{ik\Delta\omega}$, let them fitted to the four elements of sub-segments transfer matrix $m(\omega)$:

$$\sum_{k=-M}^{M} h_k^{(11)} e^{ik\Delta\omega} = m_{11} \tag{27}$$

$$\sum_{k=-M}^{M} h_k^{(12)} \, e^{ik\Delta\omega} = m_{12} \tag{28}$$

$$\sum_{k=-M}^{M} h_k^{(21)} \, e^{ik\Delta\omega} = m_{21} \tag{29}$$

$$\sum_{k=-M}^{M} h_k^{(22)} \, e^{ik\Delta\omega} = m_{22} \tag{30}$$

where $m_{11}, m_{12}, m_{21}, m_{22}$ are the elements of the 2×2 transfer matrix $m(\omega)$ in (17), which is random due to the randomness of birefringence orientation angle. Please note that the above process is just for one sub-segment filter, we need to extract many filters at the very beginning to form a filters pool for the future use.

Secondly, we randomly select a number that is assigned to a pre-extracted digital filter from filters pool for each sub-segment δz and use the selected filter as the representative of this sub-segment. Then following the above process, and we let the input signal propagates through a series of randomly selected filters that corresponds to the transfer matrices of sub-segments, and reach a distance of step size Δz:

$$U^{\Delta z} = h_k^{(\Delta z)} \cdots h_k^{(2)} h_k^{(1)} U^0 \tag{31}$$

$h_k^{(1)}, h_k^{(2)} \ldots$ represent the selected filters corresponding to each sub-segments δz, which is composed of four elements $h_k^{(11)}, h_k^{(12)}, h_k^{(21)}$ and $h_k^{(22)}$.

The next step is to undergo the dispersion effect, that is, pass through the dispersion filter $h_k^{(D)}$ as in (24):

$$\overline{U}^{\Box z} = h_k^{(D)} U^{\Delta z} \tag{32}$$

The FIR filters coefficients can be extracted:

$$h_k^{(11)} = \frac{1}{\omega_B} \int_{-\frac{\omega_B}{2}}^{\frac{\omega_B}{2}} m_{11} e^{-ik\Delta\omega} d\omega \tag{33}$$

$$h_k^{(12)} = \frac{1}{\omega_B} \int_{-\frac{\omega_B}{2}}^{\frac{\omega_B}{2}} m_{12} e^{-ik\Delta\omega} d\omega \tag{34}$$

$$h_k^{(21)} = \frac{1}{\omega_B} \int_{-\frac{\omega_B}{2}}^{\frac{\omega_B}{2}} m_{21} e^{-ik\Delta\omega} d\omega \tag{35}$$

$$h_k^{(22)} = \frac{1}{\omega_B} \int_{-\frac{\omega_B}{2}}^{\frac{\omega_B}{2}} m_{22} e^{-ik\Delta\omega} d\omega \tag{36}$$

$$h_k^{(D)} = \frac{1}{\omega_B} \int_{-\frac{\omega_B}{2}}^{\frac{\omega_B}{2}} \exp[i(\frac{\beta_2}{2}\omega^2 - \frac{\beta_3}{6}\omega^3)\Delta z] e^{-ik\Delta\omega} d\omega \tag{37}$$

At last, the nonlinear effect will be counted to accomplish one propagation step:

$$\overline{\overline{U}}^{\Box z} = \exp(\Box z N)\overline{U}^{\Box z} \tag{38}$$

The expression of N is showed in equation (13). The equations (31) and (32), together with nonlinear effect equations (38), form the split-step digital filtering method for coupled nonlinear Schrodinger equation. To cover the random effect of PMD, for each simulation we calculate the result for ten times and compute the average as its output.

Comparing with the straightforward scheme that is used to simulate the PMD effect, our proposed scheme requires less computation cost. The reason is the transfer matrices for every sub-segments are selected randomly from a large series of pre-extracted digital filters, and hence do not need to be computed at every step as in the conventional method. The pre-extracted process which requires large computation time only needs to be computed once and can be used in the following simulation. And the digital filter corresponding to the transfer matrix of every sub-segment is selected from a large number of pre-extracted filters by a Random Number Generator (RNG). Because of the above reasons, the randomness of fiber birefringence is guaranteed and the computation time is saved.

A comparison of these three schemes is plotted as following:
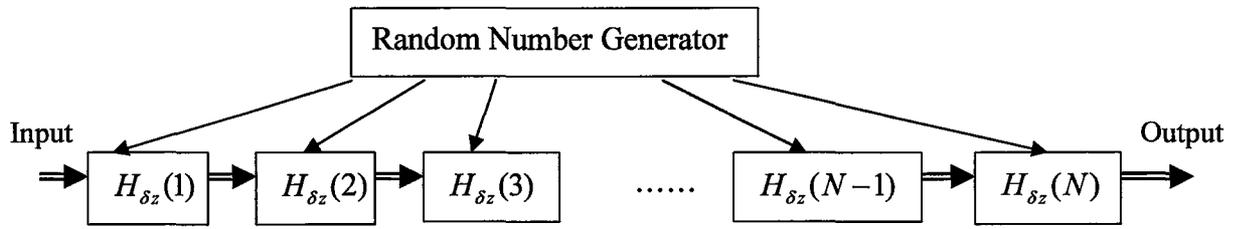
Fig. 2 Split-step FFT simulation scheme for one propagation step Δz
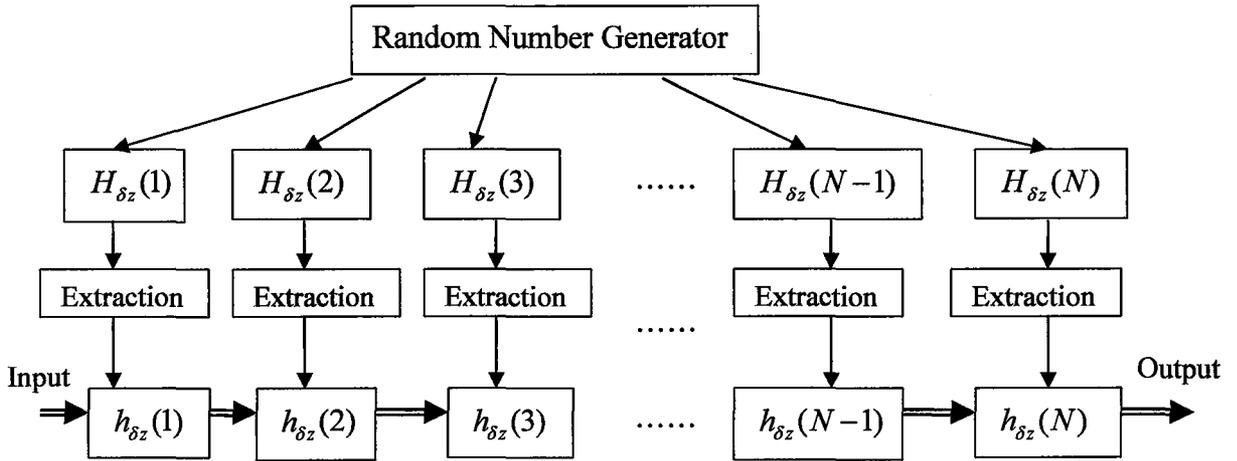
Fig. 3 Straightforward split-step time-domain simulation scheme for one propagation step Δz
Note: Assume Δz is composed of N sub-segments δz
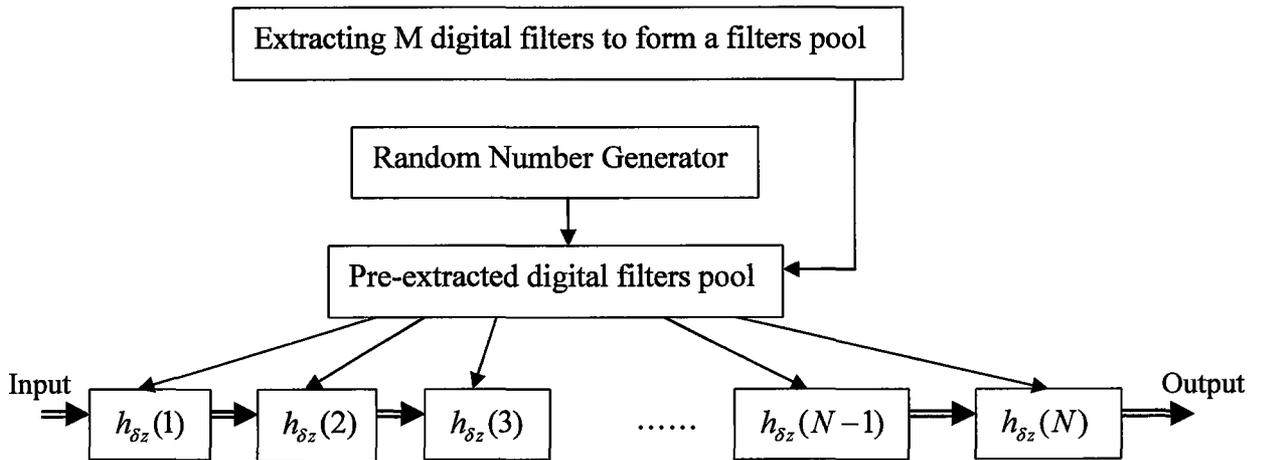
Fig. 4 Proposed split-step time-domain simulation scheme for one propagation step Δz

In the above figures, $H_{\delta z}$ is the frequency domain transfer function and $h_{\delta z}$ is the corresponding extracted digital filter. The orientation angles of $H_{\delta z}$ are randomly selected by RNG from a large number of angles. One propagation step Δz is composed of N sub-segments δz. M is the number of pre-extracted digital filters.

Assume the number of propagation steps is K and the unit extraction time spent on each digital filter is T. For the straightforward split-step time domain scheme (figure 3), the total extraction time is N*K*T. The total extraction time of our proposed split-step time domain scheme (figure 4) is M*T. For long distance propagation, it is obviously N*K*T >> M*T. We assume the number of sub-segments N is 500, the number of pre-extracted digital filters M is 200, and the propagation step K is 20. For this case, the total extraction time for straightforward scheme is N*K*T=10000*T, the total extraction time for proposed scheme is 200*T. Our proposed scheme can be 50 times faster than the straightforward scheme. With the propagation distance increases, our proposed scheme will be more efficient than straightforward scheme.

Because the propagation steps may be much larger than the number of sub-segments N, the birefringence orientation angles may repeat in the whole propagation. In order to avoid the repeated process of extracting filters coefficients, the proposed scheme (figure 4) did the extraction process in the very beginning. And the results can be used in every sub-segment propagation step δz to avoid the repeated extraction of same filters coefficients. Compared with the straightforward scheme (figure 3) which need to do the

extracting process in every sub-segment propagation step δz that may repeat extracting the same filters coefficients, the proposed scheme is obviously more computational efficient.

4.3 Comparison of Efficiency
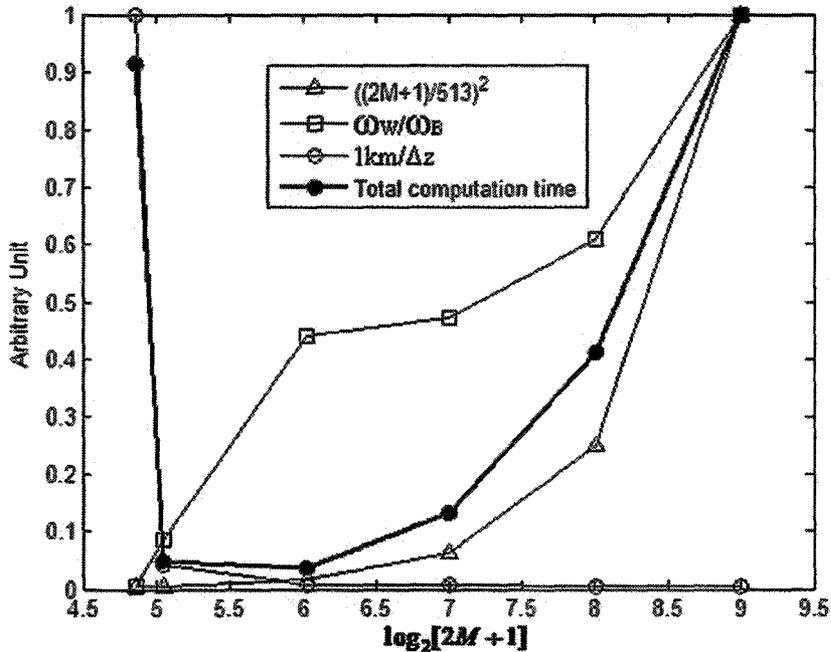
Fig. 5 Normalized filter length (Δ), normalized well-fitted bandwidth ($\Box$), propagation steps per unit length ($\Box$) at unit well-fitted bandwidth and normalized total computation time (•) as functions of filter length in logarithm scale

In figure 5, we can see that with the increasing of filter length, the well-fitted bandwidth increases. This process can either enlarge the allowed propagation step size, or reduce propagation steps per unit length. At one extreme case, the filter takes the longest length, and the corresponding well-fitted bandwidth is maximized, hence the required propagation steps per unit length are minimized [1]. At the other extreme case, the

extracted filter takes the smallest filter length, and the corresponding well-fitted bandwidth is minimized, hence the required propagation steps per unit length are maximized [10]. Because the total computation time is proportional to the product of the filtering time on each step (i.e., $O[(2M+1)^2]$) and the number of propagation steps required per unit length (i.e., $O[1/\Delta z]$), we may not get an optimized result at either extreme cases. However, we find an optimized filter length in between at which the total computation time is minimized. The reason is that the computation time on each step scales quadratically as a function of the filter length. When the filter length moves beyond a critical value, the well-fitted bandwidth doesn't increase as fast as a square function of the filter length, which makes the required propagation steps per unit length drop slower than a square function, hence the product still increases as the filter length increases. However, below this critical length, the well-fitted bandwidth drop drastically as the filter length decreases, which lead to a huge increase on the required propagation steps per unit length, hence the product appears to increase as the filter length decreases. An optimized FIR filter length is therefore observed corresponding to the turning point of the product which gives the shortest computation time. At the optimized filter length ($2M+1=65$), as much as 96% of the computation time can be saved when compared with the extreme case ($2M+1=513$).

Chapter 5

Implementation Details

When implementing the split-step digital filtering method on NSE and CNSE, some optimization steps should be taken to improve the accuracy of this method.

5.1 Half-Step Optimization Scheme

First of all, we adopt a optimized the split-step algorithm [5][15] to get a more accurate result. The nonlinear effect is calculated in the midpoint of the step size Δz, then calculating the following half step size of linear dispersion part. Derived from equations (26) and (9), this optimized algorithm for NSE can be expressed as following:

$$A_{1/2}(z+\Delta z/2,T) = \sum_{k=-M}^{M} h_k A(z,T-k\Delta) \tag{39}$$

$$\overline{A}_{1/2}(z+\Delta z/2,T) = A_{1/2}(z+\Delta z/2,T)\exp(i\Delta z \gamma e^{-\alpha z}\left|A_{1/2}(z+\Delta z/2,T)\right|^2) \tag{40}$$

$$A(z+\Delta z,T) = \sum_{k=-M}^{M} h_k \overline{A}_{1/2}(z+\Delta z/2,T-k\Delta) \tag{41}$$

Correspondingly, the fiber transfer function $\exp[i(\frac{\beta_2}{2}\omega^2 - \frac{\beta_3}{6}\omega^3)\Delta z]$ will be modified

according to half step size as $\exp[i(\frac{\beta_2}{4}\omega^2 - \frac{\beta_3}{12}\omega^3)\Delta z]$. The coefficients of FIR filter

should also be extracted according to modified fiber transfer function.

5.2 Selection of Step Size

Secondly, the split-step digital filtering method introduce an error, which is caused by the limitation on fitted phase range of fitted transfer function $\widetilde{H}_F(\omega)$ and original transfer function $\widetilde{H}_D(\omega)$. From the discussion before, we know that the fitting is actually carried out by replace the original signal by a summation of some harmonic signals [9]. Hence only a limited number of harmonic terms cannot make the fitted transfer function fully covers the original transfer function.

For a limited number of terms of fitted function $\widetilde{H}_F(\omega)$, only a limited range of phase in frequency domain can be guaranteed for an given error [1][12]. This limitation in phase range imposes limitation on step size Δz. Assume the range of phase guaranteed for a given error is Ω_e, the phase range of fitted function $\widetilde{H}_F(\omega)$ have to be smaller than original function $\widetilde{H}_D(\omega)$. By ignoring the third order dispersion, we have the following relation:

$$\frac{1}{2}\beta_2 \Delta z_{D2} \omega^2 \leq \Omega_e \tag{42}$$

In the above equation, ω is the frequency domain window width (double sides). Hence $\omega = \frac{1}{\Delta}$, where Δ is the sampling rate in time domain. We get:

$$\Delta z_{D2} \le 2\Omega_e \frac{\Delta^2}{|\beta_2|} \tag{43}$$

Considering the third order dispersion, we have the following relation from the above derivations:

$$\Delta z_{D3} \le 6\Omega_e \frac{\Delta^3}{|\beta_3|} \tag{44}$$

Equations (43) and (44) are the constraint on the step size selection from the view of second and third order dispersion, respectively.

Comparing the equations (43) and (44) with the constraint on step size selection from split-step frequency method [5]:

$$L_{D2} = \frac{T_0^2}{|\beta_2|} \tag{45}$$

$$L_{D3} = \frac{T_0^3}{|\beta_3|} \tag{46}$$

$$L_{NL} = \frac{1}{\gamma e^{-\alpha z} P} \tag{47}$$

In the above equations, L_{D2}, L_{D3} and L_{NL} are the second order dispersion length, third order dispersion length and nonlinear length, respectively. T_0 is the input pulse width. P is the peak power of the input pulse.

We can see from above that $\Delta z_{D2} < L_{D2}$ and $\Delta z_{D3} < L_{D3}$ as $\Delta \square \ T_0$. So in digital filtering method, we just need to choose the smallest value among $\Delta z_{D2}, \Delta z_{D3}$ and L_{NL} as our step size Δz.

5.3 Windowing Functions

Lastly, for further reduce the filter length of the fitted FIR filter, we introduce the windowing method on this fitted filter $\widetilde{H}_F(\omega)$ [9][12][13].

When the filter length is reduced, the Gibbs phenomenon will appear on the response of the filter [12]. Gibbs phenomenon is the oscillation effect appears on the filter response. The closer to the jump discontinuity, the bigger oscillation effect will be observed. The Gibbs phenomenon has large influence on our simulation result. The oscillation effect on the amplitude and phase of the fitted filter $\widetilde{H}_F(\omega)$ will mess up the pulse propagation result.

In order to eliminate the Gibbs phenomenon, we put windows on the extracted digital filter. The concept of windowing is a set of weighted numbers added on time domain

coefficients h_k. These weighted numbers will reduce the oscillation effect on the filter response in frequency domain [12].

Because the Gibbs phenomenon has bigger oscillation effects near the jump discontinuity of the filter response. We hence would like to extract our fitted filter from a function's amplitude with both two edges the generally fall down shape, like band-pass filter response. The reason why we do this step is the fall down shape in both edges will effectively reduce the bigger oscillation effect near the jump discontinuity of the fitted filter. In our case, the original function's amplitude is like all-pass filter response in frequency domain. So we also add a frequency domain window on the original function to make its response a band-pass filter response shape, and then extract the fitted function from this windowed original function. Hence the equations (23) and (24) would become:

$$H_F(\omega) = \sum_{k=-M}^{M} [win\_t] h_k \, e^{ik\Delta\omega} \qquad (48)$$

$$h_k = \frac{1}{\omega_B} \int_{-\frac{\omega_B}{2}}^{\frac{\omega_B}{2}} [win\_f] H_D(\omega) e^{-ik\Delta\omega} d\omega \qquad (49)$$

In the above equations, $[win\_t]$ and $[win\_f]$ represent for windowing functions added in time domain and frequency domain, respectively.

For the case in CNSE:

$$H_F^{(11)}(\omega) = \sum_{k=-M}^{M} [win\_t] h_k^{(11)} e^{ik\Delta\omega} \tag{50}$$

$$H_F^{(12)}(\omega) = \sum_{k=-M}^{M} [win\_t] h_k^{(12)} e^{ik\Delta\omega} \tag{51}$$

$$H_F^{(21)}(\omega) = \sum_{k=-M}^{M} [win\_t] h_k^{(21)} e^{ik\Delta\omega} \tag{52}$$

$$H_F^{(22)}(\omega) = \sum_{k=-M}^{M} [win\_t] h_k^{(22)} e^{ik\Delta\omega} \tag{53}$$

And,

$$h_k^{(11)} = \frac{1}{\omega_B} \int_{-\frac{\omega_B}{2}}^{\frac{\omega_B}{2}} [win\_f] M_{11} \exp(D\Delta z) e^{-ik\Delta\omega} d\omega \tag{54}$$

$$h_k^{(12)} = \frac{1}{\omega_B} \int_{-\frac{\omega_B}{2}}^{\frac{\omega_B}{2}} [win\_f] M_{12} \exp(D\Delta z) e^{-ik\Delta\omega} d\omega \tag{55}$$

$$h_k^{(21)} = \frac{1}{\omega_B} \int_{-\frac{\omega_B}{2}}^{\frac{\omega_B}{2}} [win\_f] M_{21} \exp(D\Delta z) e^{-ik\Delta\omega} d\omega \tag{56}$$

$$h_k^{(22)} = \frac{1}{\omega_B} \int_{-\frac{\omega_B}{2}}^{\frac{\omega_B}{2}} [win\_f] M_{22} \exp(D\Delta z) e^{-ik\Delta\omega} d\omega \tag{57}$$

In our simulation, the Tukey window is adopted to both windowing processes [16]. The response of Tukey window is like a band-pass filter response shape, with adjustable pass band width, which is the most desirable characteristic for the use in our simulation. It

means we can simply adjust the window's coefficient to adjust the pass band width, and hence be able to find a best result for our simulation.

The Tukey window applied in this simulation has an adjustable coefficient. This Tukey coefficient can be used to form the width of pass band of the Tukey window's response [16]. This coefficient is ranged from 0 to 1. When it equals to 0, the response would be an all-pass shape, namely, a rectangular window. With the increasing of this coefficient, the pass band width will shrink and the response of the Tukey window will become a band-pass shape. When this Tukey coefficient is increased to 1, the pass band width will be minimized. Then the Tukey window would become a Hamming window [12]. As we mentioned before, we use this feature to reduce the Gibbs phenomenon that has bigger oscillation effect near the jump continuity points. In our simulation, we scanned all the possible combination of these two Tukey coefficients to find the minimum cumulative error in a given effective bandwidth.
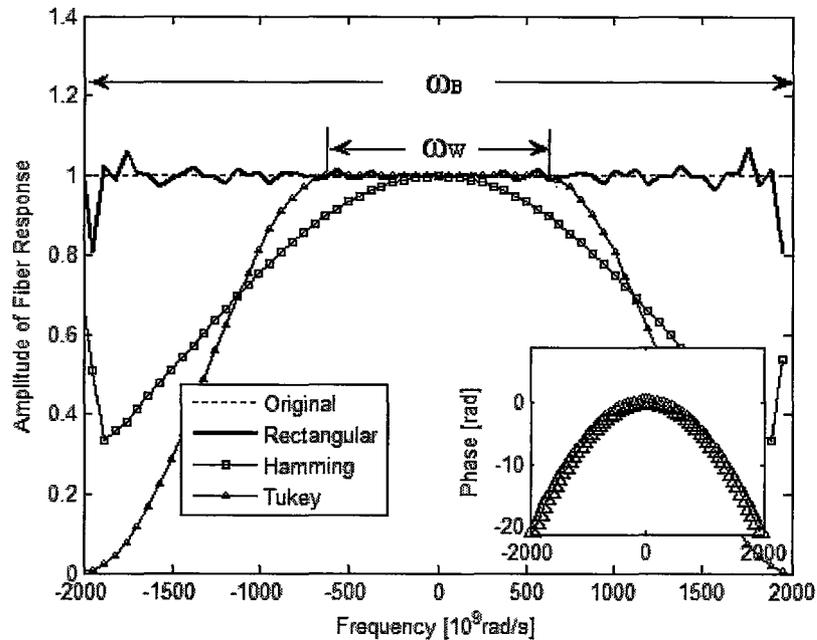
Fig. 6 Comparison on the amplitude and phase (shown as the inlet) between original fiber transfer function and extracted FIR filter response with filter length $2M + 1 = 43$ under different window functions, where ω_W is defined as the bandwidth at unit step size within which $\chi^2 \leq 10^{-6}$

Figure 6 shows the effectiveness of different windowing methods applied on the extracted FIR filter. The rectangular window gives the largest bandwidth, but has least effect on removing the Gibbs phenomenon. So the oscillation effect can be observed within the bandwidth. The Hamming window has the best effect on removing the Gibbs phenomenon, but provides the least bandwidth. The most proper window function used in our method is the Tukey window. It provides the best compromising between enlarging bandwidth and removing Gibbs phenomenon.

Chapter 6

Simulation Results

6.1 Simulation Results on NSE

In our simulation, the following parameters (G.652 SMF) are used to guarantee the reality and accuracy of the results. The center wavelength is placed around the 1550nm (C band). The second order dispersion coefficient $\beta_2 = -21.6 ps^2 / km$, and the third order dispersion coefficient $\beta_3 = 0.117 ps^3 / km$. The nonlinear coefficient is $\gamma = 2.4 W^{-1} / km$. Here, we ignore the fiber loss $\alpha = 0$. The FWHM width of input pulse is $14.7 ps$ and the signal sampling interval $\Delta = 1.5625 ps$. The step size Δz is selected as 5km. By doing an optimization process mentioned before, we choose the filter length (2M+1) as 65.

A Gaussian pulse is used as input signal to test this split-step digital filtering method. The input signal was propagated through two different distances (20km and 60km), by both the split-step frequency method and split-step digital filtering method. Because the frequency method uses the fast Fourier transformation (FFT) technique, we mark it as FFT in these figures. The digital filtering method employs FIR filter, so it is marked as FIR in all these figures.
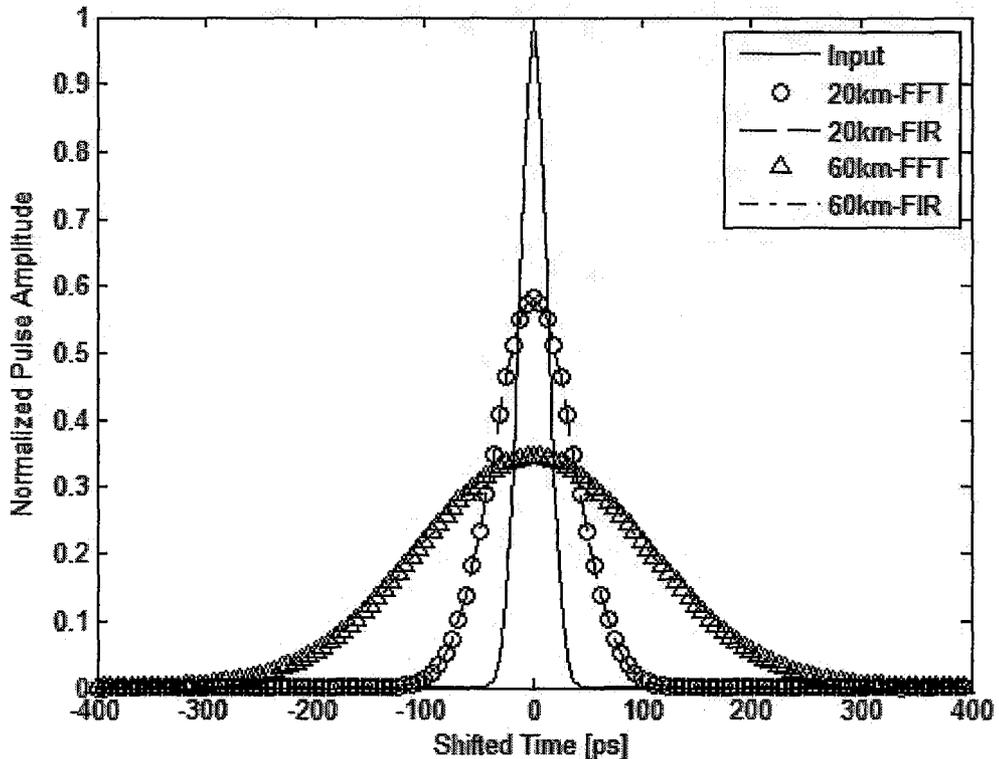
Fig. 7 A Gaussian pulse propagates through 20km and 60km. Both the frequency method and digital filtering method is used.

In the figure 7, the frequency method using FFT is treated as the benchmark for our digital filtering method. From those figures, we see that the results by split-step digital filtering method match the results by split-step frequency method exactly. The pulse is broadened as the propagation distance grows longer. It is an obvious phenomenon caused by fiber dispersion. These results perfectly match various already published results [1][5][14][15][17].
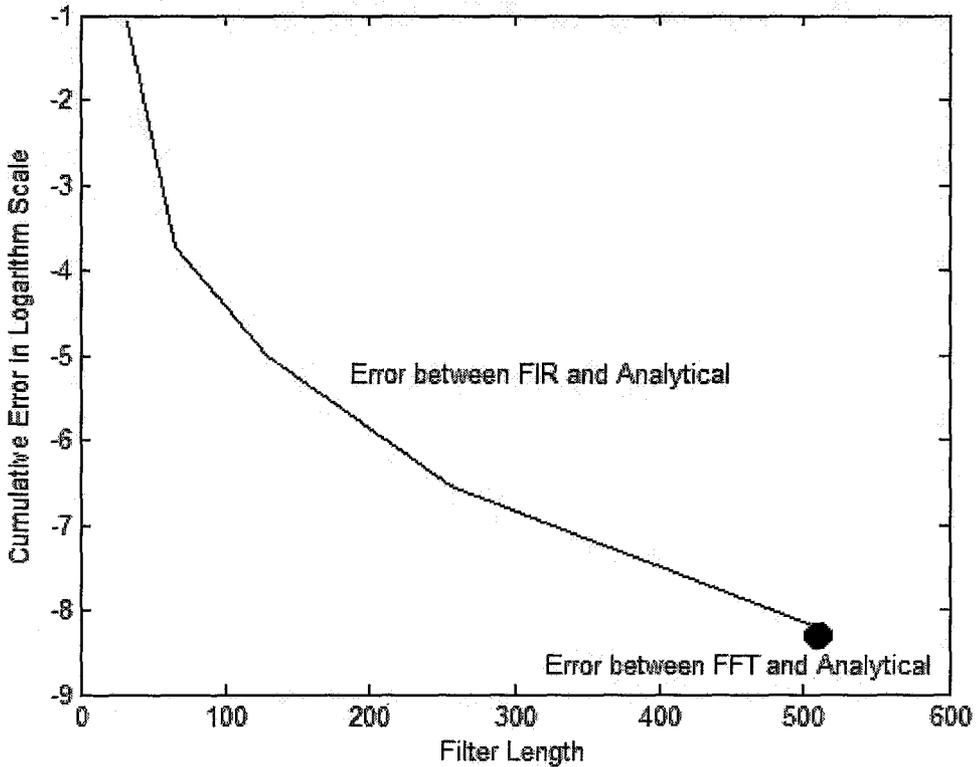
Fig. 8 Error comparison between FIR method and analytical solution and error between FFT
method and analytical solution

In figure 8, the cumulative error between FIR method and analytical solution and error between FFT method and analytical solution is plotted. Here, we only consider the second order dispersion. We set the step size of 1km and the fitted bandwidth as 1000G rad/s. From the above figure, we can observe that with the reducing of filter length, the error of FIR method is increasing. In the case of the filter length of 512, these are very small error between FIR and FFT methods, which is the similar case in [1].

To further test this optimized digital filtering method, a fiber system with strong third order dispersion is presented with zero second order dispersion. The system parameters

are showed as following: $\beta_2 = 0\,ps^2/km$, and the third order dispersion coefficient

$\beta_3 = \pm0.117\,ps^3/km$ (tested separately). The nonlinear coefficient is $\gamma = 2.4W^{-1}/km$. The

FWHM width of input pulse is $3.675\,ps$ and the signal sampling interval

$\Delta = 0.390625\,ps$. The step size is set to $\Delta z = 70km$, and a propagation distance 2100km

is adopted.

Figure 8 and Figure 9 show the pulse propagation with both the positive and negative

third order dispersion coefficients, they have good accordance with the published results

[1][5]:
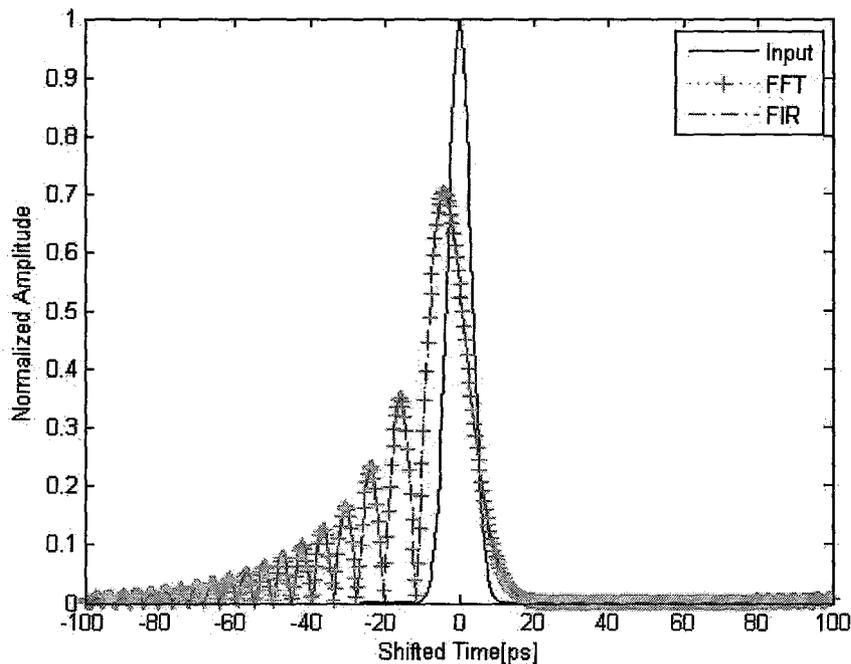
Fig. 9 A Gaussian pulse propagated with only negative third order dispersion.
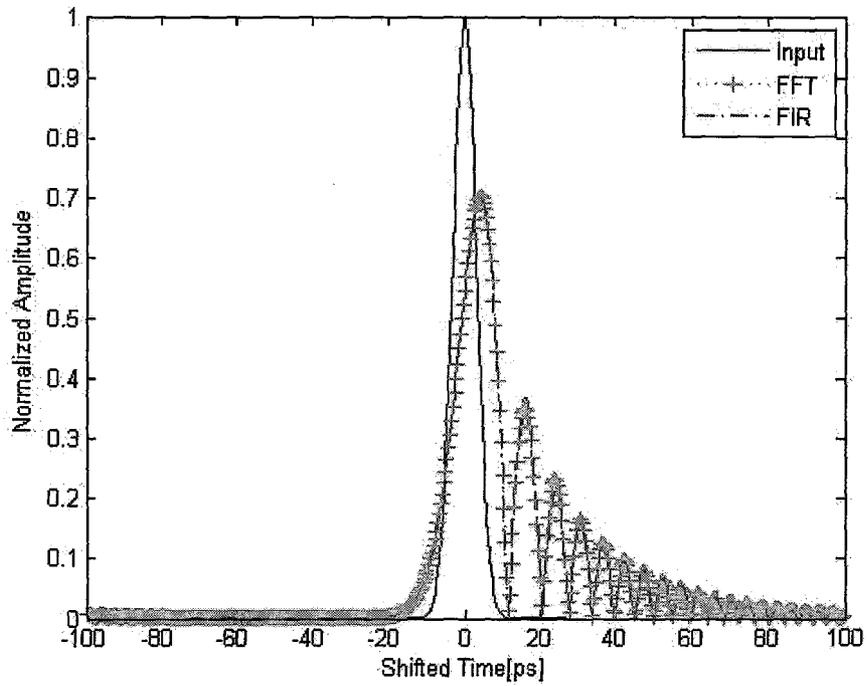
Fig. 10 A Gaussian pulse propagated with only positive third order dispersion.
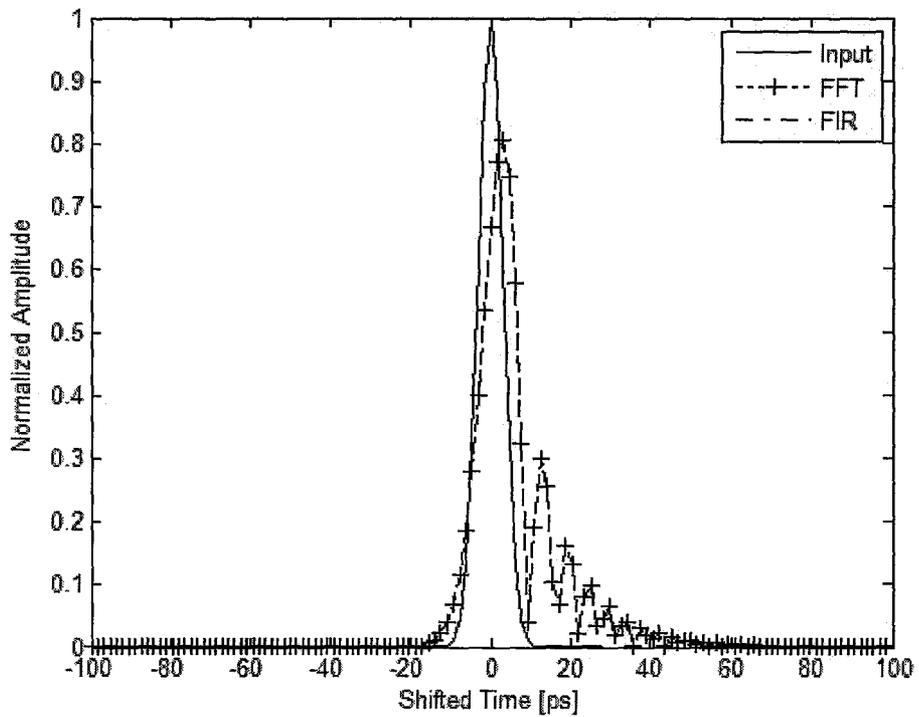
Fig. 11 A Gaussian pulse propagated with only positive third order dispersion of $0.0585 ps^3 / km$
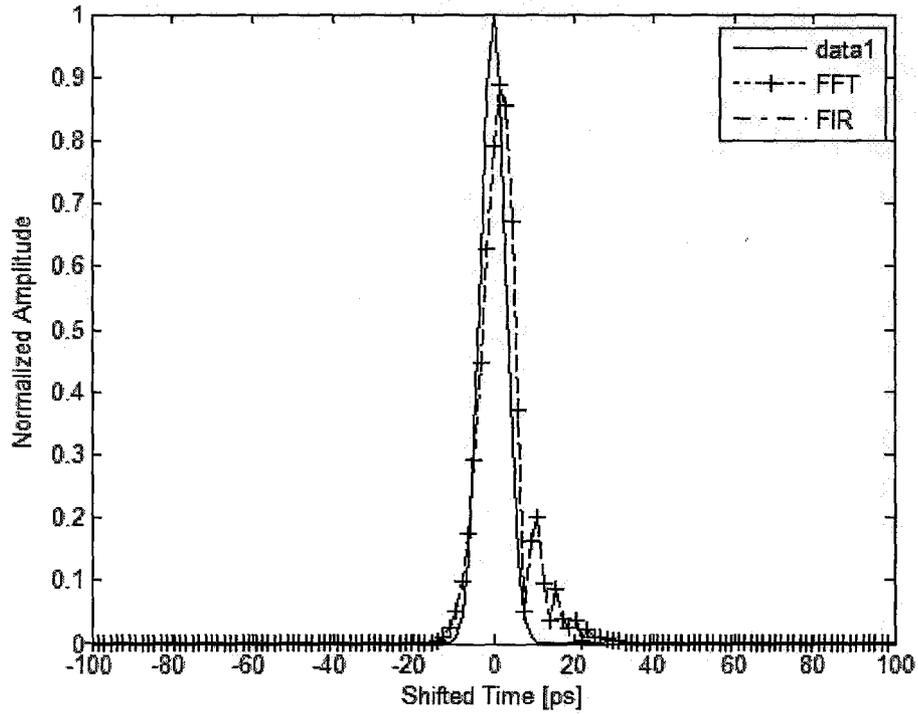
Fig. 12 A Gaussian pulse propagated with only positive third order dispersion of $0.02925 ps^3 / km$
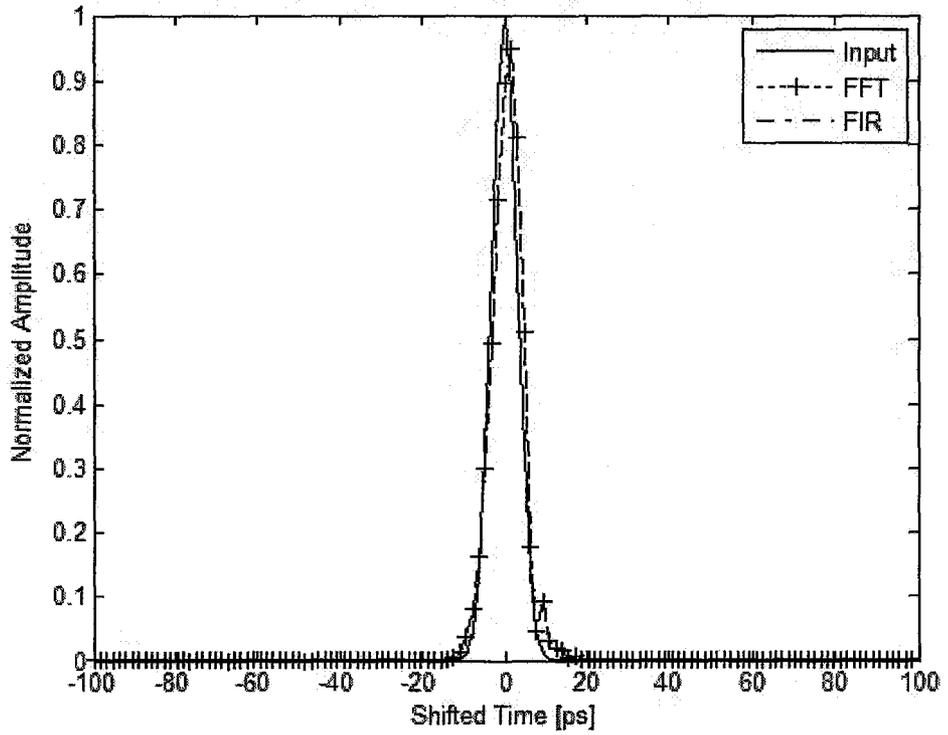
Fig. 13 A Gaussian pulse propagated with only positive third order dispersion of $0.014625\,ps^3\,/\,km$
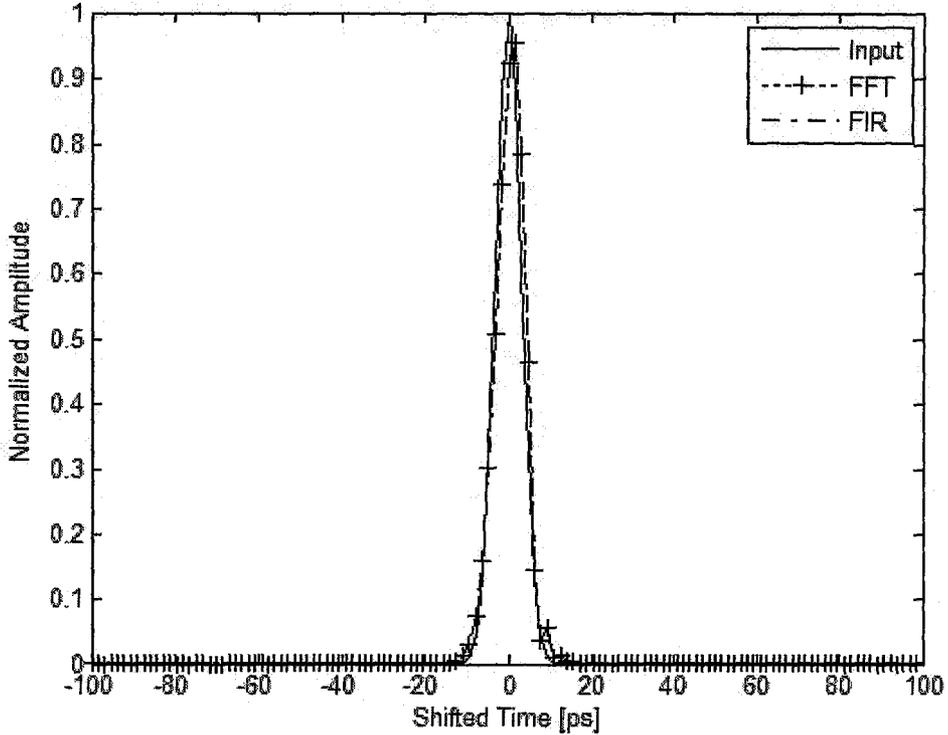
Fig. 14 A Gaussian pulse propagated with only positive third order dispersion of $0.0117 ps^3 / km$

6.2 Simulation Results on CNSE

This optimized digital filtering method is also implemented on the PMD simulation. We select the fiber PMD parameters in [2] with: fiber correlation length $L_{corr} = 100m$, beating length $\Lambda_{beat} = 50m$, and PMD coefficient $D_{PMD} = 3 ps /(km)^{1/2}$. The number of sub-segments in one step size is 500 and the FWHM width of input pulse is 28.6ps.

Following the relation $b = \dfrac{\pi}{\Lambda_{beat}}$ and $b' = \dfrac{D_{PMD}}{2(2L_{corr})^{1/2}}$ [2], we have $b = 0.0628 m^{-1}$ and $b' = 0.1061 ps /(km * m)^{1/2}$, respectively.

The propagation distances of 10km, 12km, 16km, 20km and 22km are selected to show the accuracy of our method. The input power is divided into 50:50 for two polarizations, namely, P1 and P2 in our simulation. The output signal is hence composed of the outputs of these two polarizations:

(a)   (b)
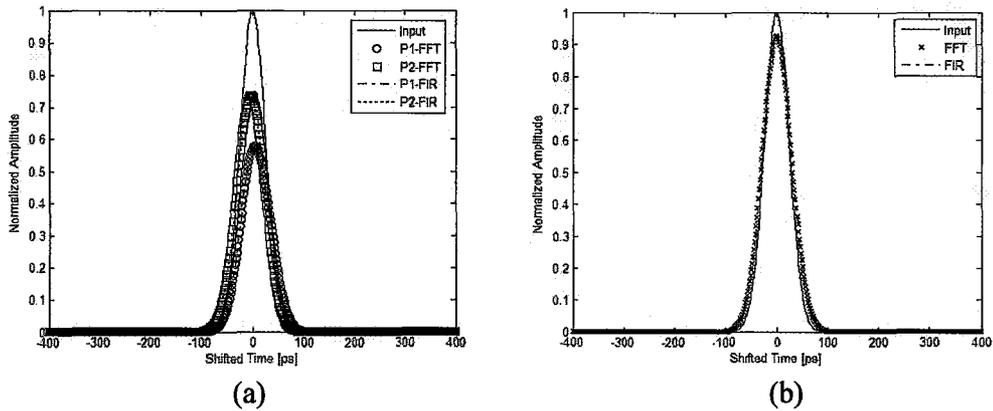
Fig. 15 Pulse propagation results of (a) two polarizations and (b) total pulse shape (P1+P2), after 10km.

(a)   (b)
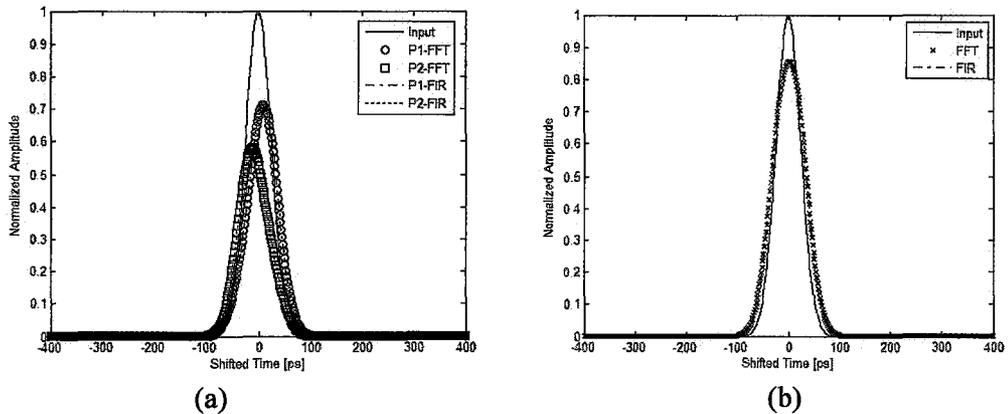
Fig. 16 Pulse propagation results of (a) two polarizations and (b) total pulse shape (P1+P2), after 12km.

(a)   (b)
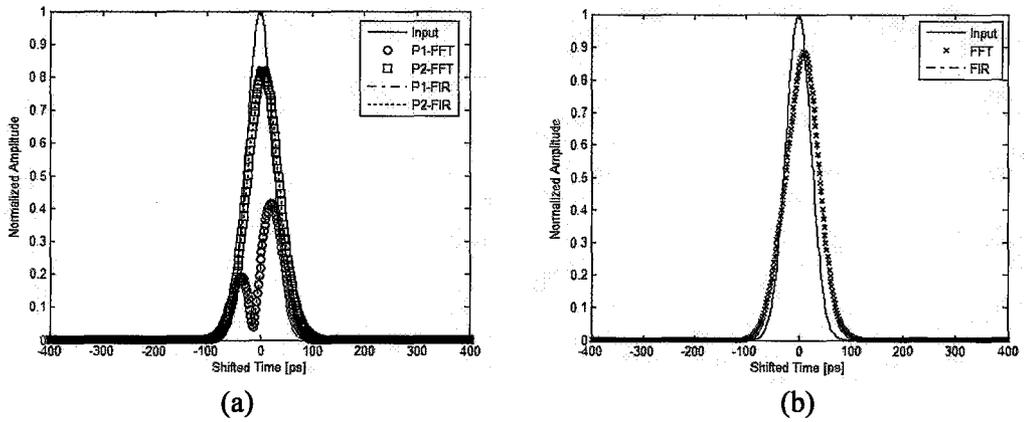
Fig. 17 Pulse propagation results of (a) two polarizations and (b) total pulse shape (P1+P2), after 16km.

(a)   (b)
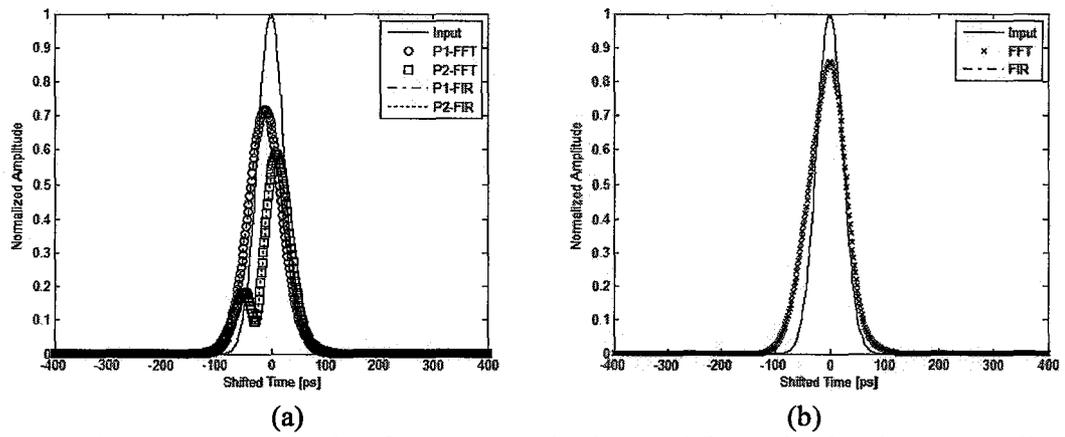
Fig. 18 Pulse propagation results of (a) two polarizations and (b) total pulse shape (P1+P2), after 20km.

(a)   (b)

48
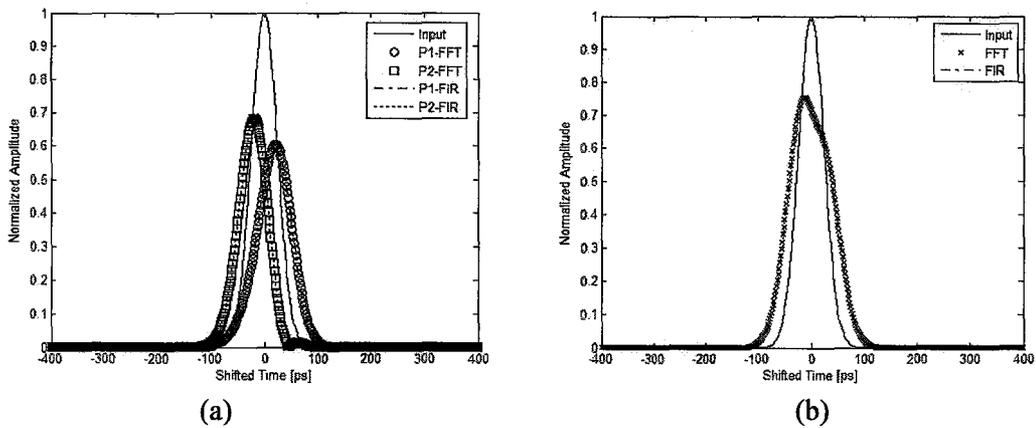
Fig. 19 Pulse propagation results of (a) two polarizations and (b) total pulse shape (P1+P2), after 22km.

In the above figures, the PMD effect is not obvious. We hence select stronger fiber birefringence strength to observe a more obvious PMD effect.

The fiber PMD coefficient is set to be $237.95 ps/km^{1/2}$ which is extremely strong in order to show the stronger PMD effect. And the width of input width is still 28.6ps in this case [18]. The propagation distances of 400m and 1.18km are selected. The simulation results are showed as below:

(a)   (b)
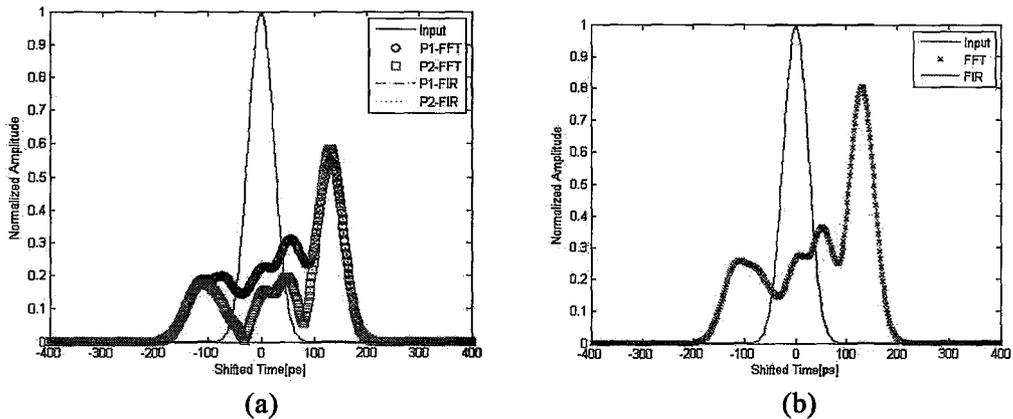
Fig. 20 Pulse propagation results of (a) two polarizations and (b) total pulse shape (P1+P2), after 400m with stronger PMD.

(a)   (b)
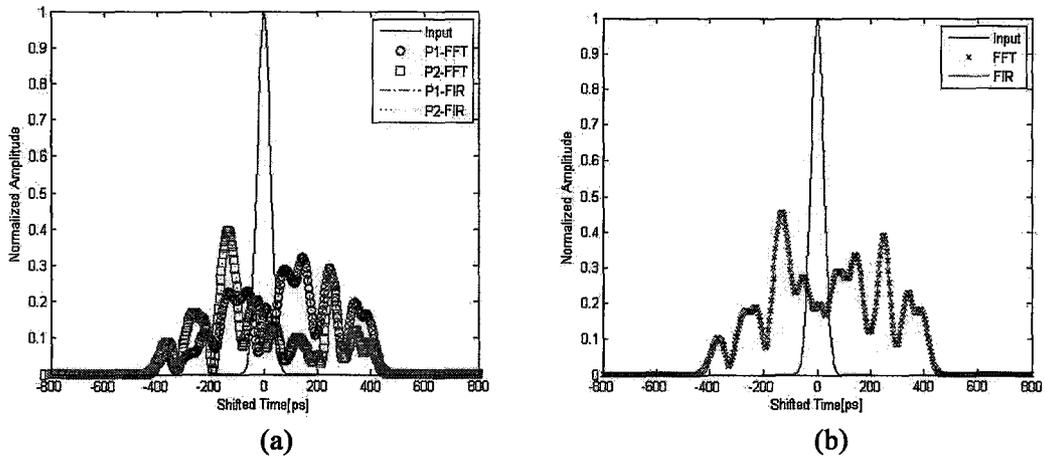
Fig. 21 Pulse propagation results of (a) two polarizations and (b) total pulse shape (P1+P2), after 1.18km with stronger PMD.
Note: In order to get more accuracy, we select a wider computation window in this simulation.

All the above PMD results show good agreement between digital filtering method and split-step frequency method using FFT.

6.3 Simulation Results on WDM system

In this section, we will show the simulation of 8 channel WDM system using both split-step frequency method and optimized digital filtering method. The system parameters are showed as following:

Operating wavelength [nm]	1547.6, 1548.4, 1549.2, 1550, 1550.8, 1551.6, 1552.4, 1553.2
Reference wavelength [nm]	1550
Channel numbers	8
Channel spacing [GHz]	100

Bit rate [Gbps]	2.5
Pulse shape	NRZ rectangular pulse with width 400 ps
Sampling interval [ps]	0.78125
Bit sequence	32 bits PRBS

Table 1 Parameters of 8 channel WDM system

The fiber parameters used are the same as the one used in our former simulation, that is, G. 652 SMF. The eye diagrams of central channel (1550nm), short edge channel (1547.6nm) and red edge channel (1553.2nm) are plotted as following figures:

(a)   (b)
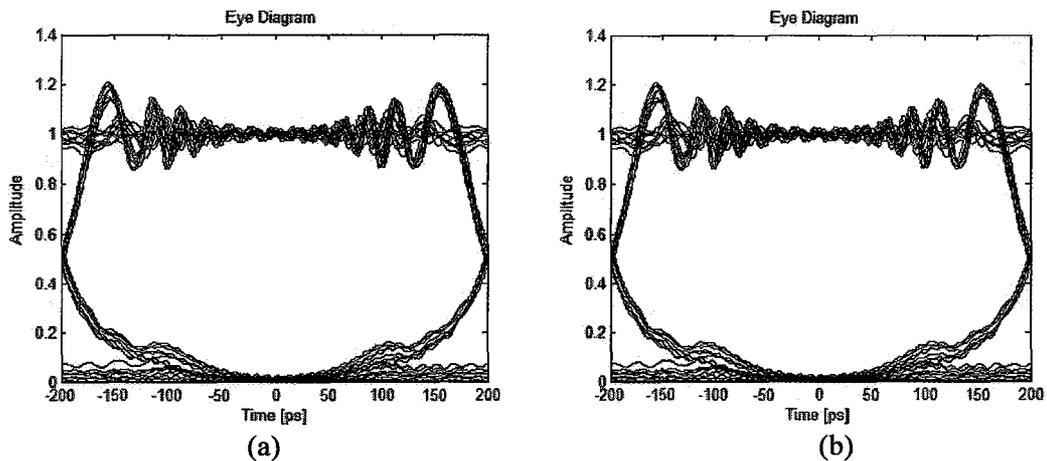
Fig. 22 The eye diagram of central channel (1550nm) after propagating 20km using both (a) split-step frequency method and (b) digital filtering method

(a)   (b)
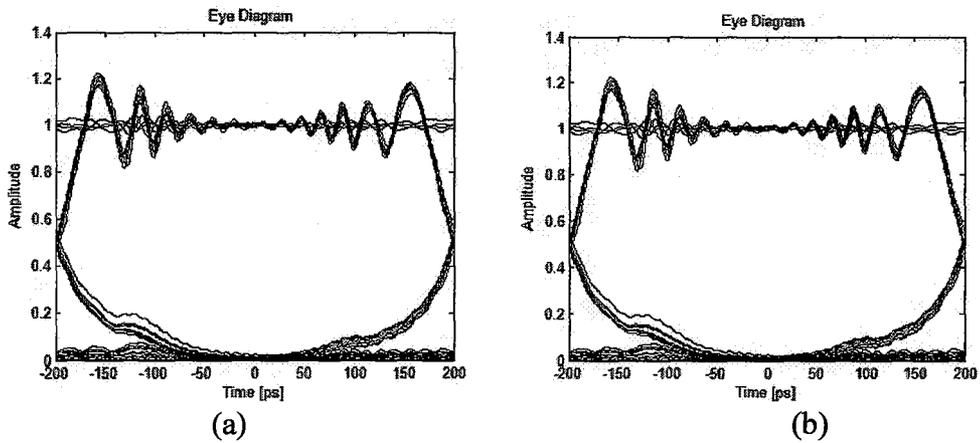
Fig. 23 The eye diagram of short edge channel (1547.6nm) after propagating 20km using both (a) split-step frequency method and (b) digital filtering method

(a)   (b)
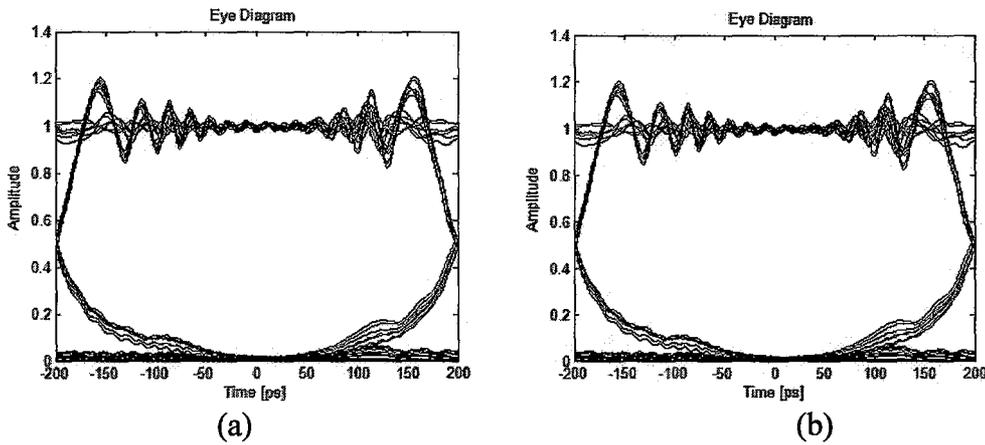
Fig. 24 The eye diagram of red edge channel (1553.2 nm) after propagating 20km using both (a) split-step frequency method and (b) digital filtering method

The next figure shows the eye diagram of central channel (1550nm) when propagating 40km:

(a)   (b)
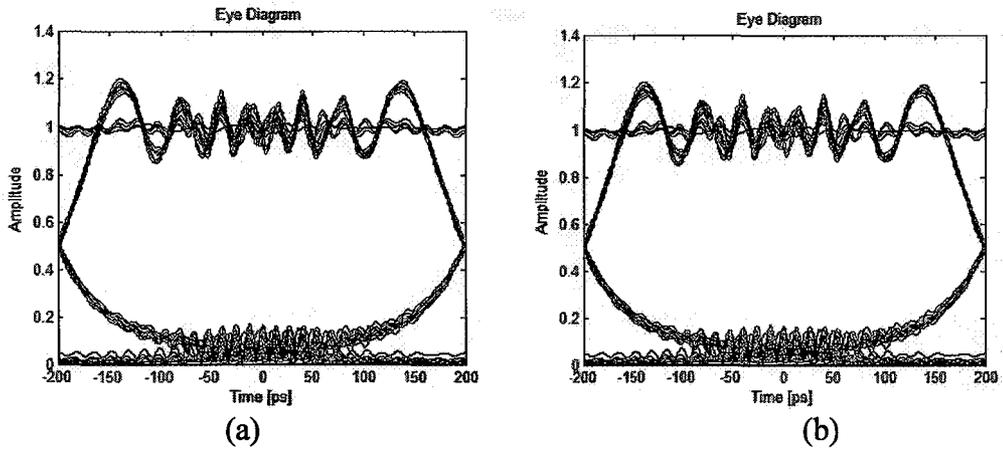
Fig. 25 The eye diagram of central channel (1550nm) after propagating 40km using both (a) split-step frequency method and (b) digital filtering method

We further adopt a system with bit rate of 5 Gbps, and the rectangular pulse width 200 ps.

The eye diagram of central channel (1550nm) after propagation 20km is showed as

following:

(a)   (b)
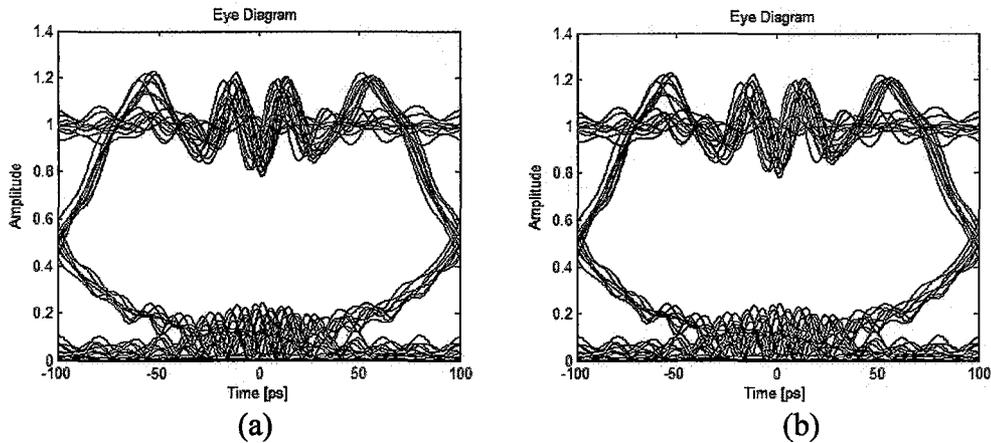
Fig. 26 The eye diagram of central channel (1550nm) after propagating 20km using both (a) split-step frequency method and (b) digital filtering method with bit rate of 5 Gbps

All the above eye diagrams show good agreement between digital filtering method and

split-step frequency method using FFT.

Chapter 7

Conclusion

7.1 Conclusion

An optimized split-step digital filtering method is proposed in this paper. The generally accepted split-step frequency method using FFT is taken as the benchmark. The results from both algorithms have good agreement for both the nonlinear Schrodinger equation and coupled nonlinear Schrodinger equation. The computation efficiency is also improved as we showed before. As a similar algorithm, this optimized digital filtering method can replace the widely used frequency domain method solver in the simulation of pulse propagation in optics fiber. The computation speed is increased compared with other split-step frequency domain methods when $2M +1 < \log N$ and former digital filtering method. A nouveau computation scheme is also proposed for the simulation of PMD effect in optic fiber. This implementation provides this digital filtering method more advantage for the simulation of various phenomenons in optics fiber.

7.2 Future Work

This optimized digital filtering method can be used to solve Schrodinger equation used in other various wave propagation simulations. In the simulation of optic device, beam propagation method (BPM) is widely used. Our proposed computation scheme can also be used to implement on the BPM and probably improves computation efficiency.

Reference

[1] X. Li, X. Chen and M. Qasmi, "A broad-band digital filtering approach for time-domain simulation of pulse propagation in optical fiber," Journal of Lightwave Technology, vol. 23, no. 2, pp. 864-875, Feb. 2005.

[2] D. Marcuse, C. R. Menyuk, and P. K. A. Wai, "Application of the Manakov-PMD equation to studies of signal propagation in optical fibers with randomly varying birefringence," Journal of Lightwave Technology, vol. 15, no. 9, pp.1735-1746, Sept 1997.

[3] C. R. Menyuk, and B. S. Marks, "Interaction of polarization mode dispersion and nonlinearity in optical fiber transmission systems," Journal of Lightwave Technology, vol. 24, no. 7, pp. 2806-2826, July 2006.

[4] R. H. Hardin, and F. D. Tappert, "Applications of the split step Fourier method to the numerical solution of nonlinear and variable coefficient wave equation," SIAM rev. Chronicle, vol. 15, p. 423, 1973.

[5] G. P. Agrawal, *Nonlinear Fiber Optics*. New York: Academic, 2001.

[6] P. K. A. Wai, W. L. Kath, C. R. Menyuk, and J. W. Zhang, "Nonlinear polarization-mode dispersion in optical fibers with randomly varying birefringence," J. Opt. Soc. Am. B, vol. 14, no. 11, pp. 2967-2979, Nov. 1997.

[7] A. Galtarossa, L. Palmieri, M. Schiano, and T. Tambosso, "Statistical characterization of fiber random birefringence," Optics Letters, vol. 25, no. 18, pp.1322-1324, Sept. 2000.

[8] P. K. A. Wai, and C. R. Menyuk, "Polarization mode dispersion, decorrelation, and diffusion in optical fibers with randomly varying birefringence," Journal of Lightwave Technology, vol. 14, no. 2, pp. 148-157, Feb. 1996.

[9] S. Mitra, *Digital Signal Processing, A Computer-Based Approach*. McGraw-Hill, 2006.

[10] A. Carena, V. Curri, R. Gaudino, P. Poggiolini, and S. Benedetto, "A time-domain optical transmission system simulation package accounting for nonlinear and polarization-related effects in fiber," Journal on Selected Areas in Communications, vol. 15, no. 4, pp.751-765, May 1997.

[11] W. H. Press, S. A. Teukolsky, W. T. Vetterling, and B. P. Flannery, *Numerical Recipes*. Cambridge, U.K.: Cambridge Univ. Press, 2001.

[12] R. W. Hamming, *Digital Filters, 3rd Edition*. Englewood Cliffs, NJ: Prentice-Hall, 1998.

[13] S. Smith, *Digital Signal Processing, A Practical Guide for Engineers and Scientists*. Newnes, Elsevier Science, 2003.

[14] M. C. Jeruchim, P. Balaban, and K. S. Shanmugan, *Simulation of Communication Systems*. Norwell, MA: Kluwer Academic, 2000.

[15] O. V. Sinkin, R. Holzlohner, J. Zweck, and C. R. Menyuk, "Optimization of the split-step Fourier method in modeling optical fiber communication systems," *J. Lightw. Technol.*, vol. 21, no. 1, pp. 61–68, Jan. 2003.

[16] Harris, F. J. "On the use of windows for harmonic analysis with the discrete Fourier transform." Proceedings of the IEEE. vol. 66, pp. 66-67. Jan. 1978.

[17] G. P. Agrawal, *Fiber-Optic Communication Systems*. John Wiley & Sons, Inc, 2002.

[18] T. Ning, Z. Tan, Y. Liu, and S. Jian, "24.3-ps Gaussian pulse transmission over ultrahigh-PMD fiber," Optics Express, vol. 11, Issue 19, pp. 2364-2369, Sept. 2003.

[19] M. Akbulut, L. Xu, A. M. Weiner, and P. J. Miller, "Wideband all order PMD compensation via pulse shaping," OFC Conference Technical Digest, vol.6, pp. 3, March 2005.

[20] T. Kremp, and W. Freude, "Fast split-step wavelet collocation method for WDM system parameter optimization," Journal of Lightwave Technology, vol. 23, no. 3, pp. 1491-1502, March 2005.

[21] A. Lowery, O. Lenzmann, I. Koltchanov, R. Moosburger, R. Freund, A. Richter, S. Georgi, D. Breuer, and H. Hamster, "Multiple signal representation simulation of photonic devices, systems, and networks," *IEEE J. Select. Topics Quantum Electron.,* vol. 6, no. 2, pp. 282-296, Mar. 2000.

[22] C. R. Menyuk, "Application of multiple-length-scale methods to the study of optical fiber transmission," Journal of Engineering Mathematics, 36: pp. 113-136, 1999.